Hyperspectral imaging technology for determination of dichlorvos residue on the surface of navel orange

Jing Li (黎 静)[1], Long Xue (薛 龙)[2], Muhua Liu (刘木华)[1*], Xiao Wang (王 晓)[1], and Chunsheng Luo (罗春生)[1]

[1]*School of Engineering, Jiangxi Agricultural University, Nanchang 330045, China*

[2]*School of Mechanical and Electronical Engineering, East China Jiaotong University, Nanchang 330013, China*

[*]*E-mail: suikelmh@sohu.com*

Received April 19, 2010

A hyperspectral imaging system is developed to detect dichlorvos residue on the surface of navel orange. After acquiring hyperspectral images of 400 navel oranges, the actual content of dichlorvos residue is measured by gas chromatography. Optimal wavelengths are extracted using the regression coefficients of partial least squares (PLS), and a PLS model with 12 factors is established. In the prediction set of 0.2282−11.652-mg/kg pesticide residue, the correlation coefficient and the root mean standard error are 0.8320 and 1.3416, respectively. The hyperspectral imaging technology can meet the requirement of online fast nondestructive detection.

OCIS codes: 110.4234, 300.6490, 100.2000.

doi: 10.3788/COL20100811.1050.

The regulation of pesticide usage has become an important human health issue because of the possibility of contracting various diseases caused by pesticide on fruits or vegetables in the food chain. The amount of pesticide residue on products is usually measured using conventional techniques such as gas chromatography (GC) and high-performance liquid chromatography (HPLC). The use of conventional analyses for detecting pesticide residues in all product lines is becoming impossible because of the limitations of time and labor[1]; therefore, utilizing these conventional analyses has been somewhat disadvantageous. Spectroscopy technologies such as near infrared spectroscopy and fluorescence spectroscopy, in combination with the advance in chemometrics, have extended their uses to industrial and agricultural areas[2,3]. Such technologies have been proven useful for measuring internal quality attributes such as total soluble solid content of apple[4], sugar content in strawberry[5], catechins content in tea[6,7], meat and bone meal content in fishmeal[8], and firmness of pear[9]. However, compared with the hyperspectral imaging technology, these spectroscopic methods have a drawback because the spectral data are acquired from a single point or from a small portion of the tested sample. In contrast, hyperspectral imaging has the advantage of receiving spatially distributed spectral responses at each pixel of a fruit image. Moreover, the technology has been implemented in several applications, such as determining internal quality of strawberry[10], fecal detection on poultry carcasses[11], and detecting pesticide residue on navel orange surface[12].

Navel orange, is known not only as a fresh fruit but also as a processed product. The main aim of this letter is to develop a hyperspectral imaging system and open up a new nondestructive method of dichlorvos residue determination. Partial least square (PLS) models are built to predict dichlorvos residue on the surface of navel orange quantitatively using hyperspectral images. Based on the regression coefficients of PLS, optimal wavelengths are selected, and new PLS models are built.

Four hundred navel oranges were purchased from the Nongda Market in Nanchang, Jiangxi, China. Firstly, these navel oranges were washed and air-dried. Next, different concentrations of dichlorvos solutions were sprayed on different groups of navel oranges to obtain different concentrations of dichlorvos residue. The samples were kept in the laboratory for 10−11 h to dry the surfaces. Subsequently, spectra were acquired using the hyperspectral imaging system. Finally, dichlorvos residue on the surfaces of samples was measured by GC (SP-6890, Lunan Rui Hong Chemical Co., Ltd., China) the next day.

Hyperspectral images were acquired by hyperspectral imaging system (Fig. 1), composed of a line-scan spectrograph (ImSpector, V10E, Spectra Imaging Ltd., Finland), a complementary metal-oxide semiconductor (CMOS) camera (MV-D1024E-40-U2, Photonfocus AG, Switzerland), an illumination unit with 4 halogen lamps (50 W), and a computer. Spectrograph-measured reflectance spectra at a wavelength range of 400−1000 nm and exposure time adjusted to 50 ms were adopted throughout the whole experiment. The distance between the lens and the surface of the navel orange image was fixed at 600 mm. Before data acquisition, the hyperspectral imaging system was corrected with a

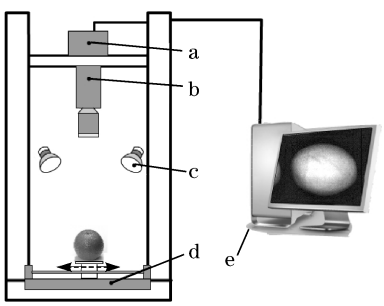

Fig. 1. Schematic of hyperspectral imaging system. a: CMOS camera, b: spectrograph with a standard C-mount zoom lens, c: halogen lighting unit, d: conveyer, e: computer.

white standard (SRT-99-100, Labsphere, Inc., USA) and a dark reference.

The preprocessing procedures taken for the sample were as follows. 1) Ten grams of navel orange skin were placed in high-speed tissue crushing machine with ethyl acetate; 2) after crushing the navel orange skin, the machine was thrice washed with approximately 30-ml ethyl acetate; 3) the mixed solution was filtered with filter paper; 4) the filtrate was concentrated using a rotary evaporator until almost dry, then the residue was diluted with acetone to 5 ml; 5) the solution was filtered with a membrane of 0.45 μm for testing.

The amount of dichlorvos in the solution was measured by gas chromatography. The capillary column for GC analysis was a 0.53 mm×30 m column with 1.0-μm particles. The GC was operated under the following conditions: injection volume is 1 μL; injector temperature, flame ionized detector (FID) temperature and columm temperature are 200, 180, and 140 °C, respectively; the velocities of N_2, air, and H_2 are 36, 128, and 15 mL/min, respectively. Trial measurements were performed for each sample.

Figure 2 shows a typical chromatogram obtained under the above-mentioned conditions. The peak time for dichlorvos is approximately 3.7 min, with the dichlorvos quantitatively determined by the peak area of the chromatogram. The dichlorvos content of the samples can be precisely calculated by the linear relation of the content, as well as the peak area between the dichlorvos of the samples and the standard solution.

The hyperspectral images were processed using Software ENVI. A reflection area was found and marked in each image. To calculate the spectral reflection, a region of interest (ROI) was defined as the pixel area obtained by taking out the marked reflection area from the total area of a navel orange in an image. The mean reflectance spectrum of a ROI was calculated by averaging the spectral response of each pixel in the ROI. 400 mean reflectance spectra were calculated, with each spectrum including spectral information from 400 to 1000 nm.

Software Unscrambler (CAMO, Oslo, Norway) was used for all calculations. PLS regression was performed to develop a calibration equation from the spectra of samples based on the spectral preprocessing technique of multiplicative scatter correction (MSC). Model performance was compared in terms of root mean standard error of calibration (RMSEC), root mean standard error of prediction (RMSEP), and correlation coefficient (R) between the predicted and the measured values.

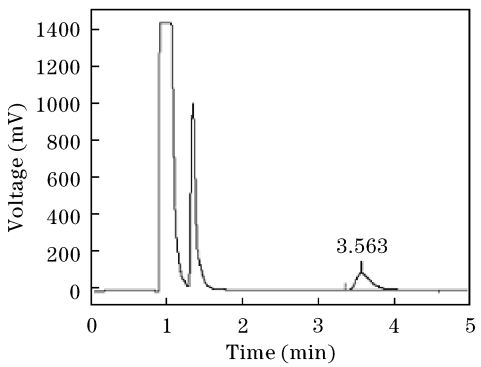

Fig. 2. Typical chromatogram of dichlorvos obtained by GC.

The dichlorvos residue measurements (n = 400) were normally distributed around the mean (max = 12.093 mg/kg, min = 0.1972 mg/kg). The 400 samples were ordered according to the ascending order of dichlorvos residue measurements. From the 1st to 390th sample, every three samples were considered as a group. The 2nd sample of each group was chosen as the sample of the prediction set, and the remaining samples were chosen as samples of the calibration set. Therefore, the calibration set included the maximum and the minimum dichlorvos residue measurements. Moreover, the calibration set included 270 data and prediction set included 130 data (Table 1). Table 1 shows the descriptive statistics for dichlorvos residue of navel oranges determined by GC.

Figure 3 shows the mean reflectance spectra in a range of 400–1000 nm collected from the navel oranges. Clearly, larger noise is found at the lower (400–499 nm) and higher (923–1000 nm) ends of the spectra dataset. Therefore, these two spectral ranges are cut from the spectra dataset. The spectra wavelength ranging of 500–922 nm is discussed in the following.

Table 1. Reference Measurements and Sample Numbers in Calibration and Prediction Sets

Set	Number of Samples	Mean Value (mg/kg)	Range (mg/kg)
Calibration	270	3.1788	0.1972−12.0932
Prediction	130	3.3913	0.2282−11.6520

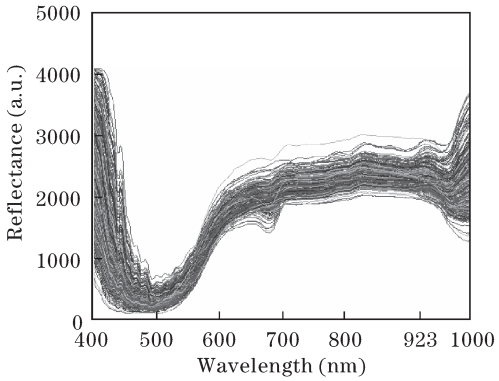

Fig. 3. Mean reflection spectra of navel oranges.

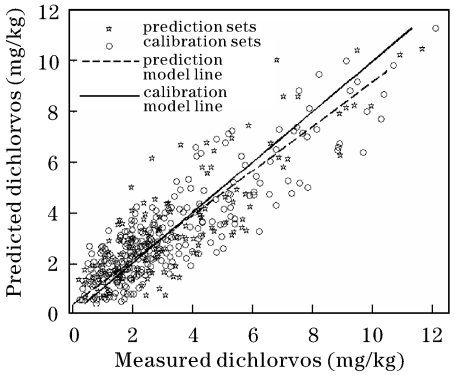

Fig. 4. Measured and predicted dichlorvos residues of calibration and prediction sets using 16 latent factors.

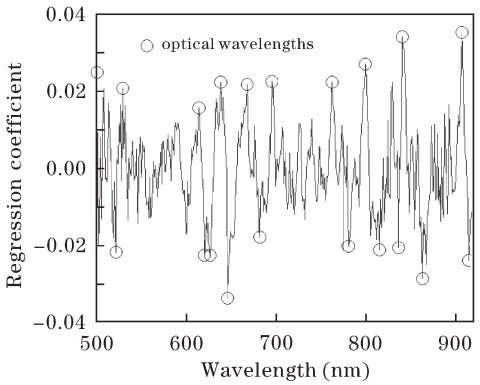

Fig. 5. Optimal wavelengths based on the regression coefficients of PLS.

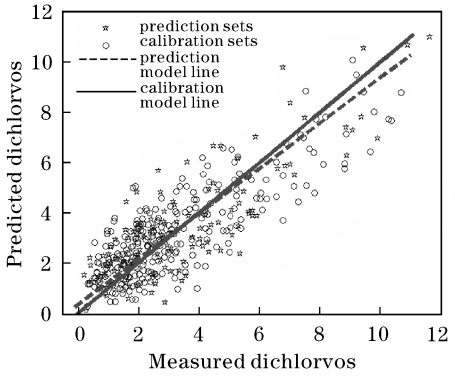

Fig. 6. Measured and predicted dichlorvos residues of calibration and prediction set using optimal wavelengths and 12 latent factors.

The PLS calibration model was established using the mean spectra from 270 navel oranges of the calibration set in the spectral range consisting of 403 wavebands. The model was validated using the mean spectra of 130 navel oranges in the prediction set. The optimal number of latent factors used in the PLS model was 16. The measured values of pesticide residue by GC and the predicted values resulting from PLS model are shown in Fig. 4. The model is found to be suitable for predicting pesticide residue of dichlorvos with R of 0.8760 and 0.8470 for calibration and prediction sets, respectively. RMSEC and RMSEP are 1.1043 and 1.3028 for the calibration and prediction sets, respectively.

Figure 5 shows the relation curve between the wavelengths and the regression coefficients of PLS, with the extracted wavelengths corresponding to the highest absolute values of regression coefficients in the curve in spite of their signs. Therefore, the optimal wavelengths were determined to be 500, 521, 528, 614, 620, 626, 639, 646, 668, 682, 696, 763, 781, 800, 815, 837, 841, 863, 907, and 915 nm. The optimal wavelengths were used to build another PLS model between the reflectance at these wavelengths and the measured dichlorvos residue; the accuracy of the PLS model is shown in Fig. 6. The performance of the model is evaluated at R, RMSEC, and RMSEP. The R value of the calibration set is 0.8407 with RMSEC of 1.2398, and that of the prediction set is 0.8320 with RMSEP of 1.3416.

Compared with the first PLS model (with 403 wavebands), the second PLS model (with 20 wavelengths) has slightly lower performance in prediction in terms of R, RMSEC, and RMSEP; however, the number of wavelengths used to establish PLS model decreases to 20, with the latent factor of 12.

The study has indicated the possibility of developing a nondestructive technology using hyperspectral imaging for measuring pesticide residue of dichlorvos on the surface of navel orange. Two types of PLS models have been established: one is based on the whole spectral range (500–922 nm), including 403 wavebands and 16 latent factors, and the other is based on 20 optimal wavelengths extracted using regression coefficients from the PLS model and 12 latent factors. Comparison of the two models has shown that both models determine dichlorvos residue efficiently, although the second one has slightly lower performance in prediction in terms of R, RMSEC, and RMSEP. However, the second one, based on the fewer wavelengths and latent factors, will spend less time in calculation, which is very important in product lines. In the prediction set of 0.2282–11.652-mg/kg pesticides residue, the R and the root mean standard error are 0.8320 and 1.3416, respectively. The detection limit is lower than that of GC; however, this detection technology has the obvious advantages of quick and nondestructive on-line detection. In addition, the detection limit can achieve ordinary rapid detection and can be improved in further studies. In conclusion, the experimental results suggest that hyperspectral imaging can be used to determine pesticide residues on fruit surface.

This work was supported in part by the National Natural Science Foundation of China (No. 30760101), the Program for New Century Excellent Talents in University (No. NCET-09-0168), the Jiangxi Provincial Department of Science and Technology (No. 2009BNB 05705), and the Jiangxi Provincial Department of Education (No. GGJ08513).

References

1. S. Satanwong and S. Kawano, J. Near Infrared Spectrosc. **13,** 169 (2005).
2. J. Wang, G. Chen, T. Zhu, S. Gao, B. Wei, and L. Bi, Chin. Opt. Lett. **7,** 1058 (2009).
3. D. Han and J. Wang, Chinese J. Lasers (in Chinese) **35,** 1123 (2008).
4. J. Wang and D. Han, Spectroscopy and Spectral Analysis (in Chinese) **28,** 2308 (2008).
5. J. Shi, X. Zou, J. Zhao, and X. Yin, Journal of Anhui Agri. Sci. (in Chinese) **37,** 5752 (2009).
6. Q. Chen, J. Zhao, J. Cai, and V. Saritporn, Acta Opt. Sin. (in Chinese) **28,** 669 (2008).
7. Q. Chen, Z. Guo, J. Zhao, and Q. Ouyang, J. Infrared Millim. Waves (in Chinese) **28,** 357 (2009).
8. X. Zhan, L. Han, X. Liu, and Z. Yang, Acta Opt. Sin. (in Chinese) **29,** 2800 (2009).
9. Y. Zeng, C. Liu, X. Sun, X. Chen, and Y. Liu, Transactions of the CSAE (in Chinese) **24,** 250 (2008).
10. M. Nagata, J. G. Tallada, T. Kobayashi, and H. Toyoda, in *Proceedings of American Society of Agricultural Engineers* 053131 (2005).
11. G. W. Heitschmidt, B. Park, K. C. Lawrence, W. R. Windham, and D. P. Smith, Transactions of the ASABE **50,** 1427 (2007).
12. L. Xue, J. Li, and M. Liu, Acta Opt. Sin. (in Chinese) **28,** 2277 (2008).